

## Robustness of Gabor Feature Parameter Selection

J.-K. Kamarainen\*, V. Kyrki, and H. Kälviäinen  
 Laboratory of Information Processing,  
 Lappeenranta University of Technology

## Abstract

Gabor filters have been successfully used for feature extraction in many machine vision applications. In this study Gabor filtering based features are analyzed in terms of filter parameters to provide new insight into advantages of Gabor filters. Analytical and experimental results show that filter responses behave in a stable manner even while the parameter selection is suboptimal. In addition, restrictions are given for discrete domain filtering to expand continuous domain results for practical applications.

There are no general methods for the selection of Gabor filter parameters, which is often a vague and application dependent task. Thus, behavior of filters in terms of parameters provides an important piece of knowledge. Considerations of performing the filtering in discrete domain are often neglected, while in this paper they are claimed to have an important impact.

## 1 Introduction

Feature extraction methods for computer vision tasks have received a great amount of attention in image processing research. However, robustness considerations of features are often neglected, which can be hazardous for higher level analysis or the target application. In industrial applications each component of a machine vision system should behave smoothly in order to retain the robustness.

Since Daugman suggested the use of 2-D Gabor elementary functions as accurate models of the cortical simple cells in the mammalian visual system, Gabor filters have successfully been applied to various low-level computer vision tasks such as edge and line detection [3, 11] and texture segmentation [1, 5], and to applications, e.g., face recognition [2], character recognition [4], and wood defect inspection [10]. Authors have introduced two classes of Gabor filtering based features: global Gabor features [8, 9] and fundamental frequency Gabor features [6], which have been shown to be accurate and noise tolerant in applications [7].

In this paper, practical constraints are first proposed for the filtering in the discrete domain. Then, the stability of Gabor features is analyzed in terms of filtering parameters. Behavior of filters is analytically studied for an elementary function representing a non-periodic feature and the theoretical results are verified in practical experiments on symbol images. Both theoretical and experimental results indicate that stable low-level features can be constructed using the Gabor filter-

ing, and thus, robust applications can be implemented based on Gabor features.

## 2 Gabor Features

In the spatial domain, a two-dimensional Gabor filter is a complex sinusoidal plane wave modulated by a Gaussian

$$\psi(x, y) = \underbrace{e^{-(\alpha^2 x'^2 + \beta^2 y'^2)}}_{\text{Gaussian envelope}} \underbrace{e^{j2\pi f x'}}_{\text{sinusoid}}, \quad (1)$$

$$x' = x \cos \theta + y \sin \theta,$$

$$y' = -x \sin \theta + y \cos \theta,$$

and in the frequency domain, a Gaussian centered at  $(f \cos \theta, f \sin \theta)$

$$\Psi(u, v) = \frac{\pi}{\alpha\beta} e^{-\pi^2 \left( \frac{(u \cos \theta + v \sin \theta - f)^2}{\alpha^2} + \frac{(u \sin \theta - v \cos \theta)^2}{\beta^2} \right)}. \quad (2)$$

$f$  represents the frequency of the plane wave,  $\theta$  is the anti-clockwise rotation of the Gaussian envelope and the plane wave,  $\alpha$  the sharpness of the Gaussian along the axis parallel to the wave, and  $\beta$  sharpness along the axis perpendicular to the wave.

Response of the Gabor filter (1) for an image  $\xi(x, y)$  can be calculated via the convolution

$$\text{resp}_\xi(x, y) = \psi(x, y) * \xi(x, y). \quad (3)$$

$\alpha$  and  $\beta$  can be substituted by two normalization factors  $\gamma = \frac{f}{\alpha}$  and  $\eta = \frac{f}{\beta}$  [6] to form a normalized response

$$r_\xi(x, y) = \frac{f^2}{\pi\gamma\eta} \psi(x, y) * \xi(x, y). \quad (4)$$

Gabor filters in the discrete domain (images  $\xi(x, y)$  of size  $M \times N$ ) need certain restrictions for consistent results with theories in the continuous domain. The most obvious restriction is the Nyquist frequency, but in addition, the discrete Gabor filter should also have a negligible response above the Nyquist frequency. A proper construction of the filter can be accomplished by stating a percentage  $p_f$  of the filter envelope that must lie within the Nyquist limit ( $f_N = 0.5$ ) which can be approximated using the integration

$$\iint_{-0.5}^{0.5} \Psi(u, v) du dv \geq p_f \iint_{-0.5}^{0.5} \Psi(u, v) du dv \Leftrightarrow$$

$$\iint_{-0.5}^{0.5} \frac{\pi}{\alpha\beta} e^{-\pi^2 \left( \frac{(u \cos \theta + v \sin \theta - f)^2}{\alpha^2} + \frac{(u \sin \theta - v \cos \theta)^2}{\beta^2} \right)} du dv$$

$$\geq p_f. \quad (5)$$

\*Address: P.O. Box 20, FIN-53851 Lappeenranta, Finland.  
 {Joni.Kamarainen,Ville.Kyrki,Heikki.Kalviainen}@lut.fi.

Now, (5) ensures a proper filter construction in the frequency domain, but since the Gabor filters have infinite support in spatial domain, a proper spatial domain construction must be conducted as well. The minimum spatial size  $n_{min}$  can be approximated from

$$\iint_{-\frac{n_{min}}{2}}^{\frac{n_{min}}{2}} |\psi(x, y)| dx dy \geq p_s \iint_{-\infty}^{\infty} |\psi(x, y)| dx dy \Rightarrow \operatorname{erf}\left(\alpha \frac{n_{min}}{2}\right) \operatorname{erf}\left(\beta \frac{n_{min}}{2}\right) \geq p_s \quad (6)$$

to include at least  $p_s$  percent of the filter envelope inside a rectangular filter of size  $n_{min} \times n_{min}$  where  $n_{min} \leq \min(M, N)$  for an image of size  $M \times N$ . Due to the equivalence of Fourier domain multiplication and circular convolution, the Gabor filter responses are invalid near the edges of an image where the distance to the edge is below

$$\frac{n_{min}}{2}. \quad (7)$$

### Robustness

Robustness of the parameter selection can be analyzed by examining the normalized response (4) for a 2-D rectangle in terms of the Gabor filter parameters. A 2-D rectangle function of width  $w_1$ , length  $w_2$ , and unit value

$$\Pi(x, y) = \begin{cases} 0, & |x| > \frac{w_1}{2} \text{ or } |y| > \frac{w_2}{2} \\ 1, & |x| \leq \frac{w_1}{2} \text{ and } |y| \leq \frac{w_2}{2} \end{cases}, \quad (8)$$

can be considered to represent a non-periodic feature. Now, the 2-D Gabor filter aligned along the x-axis ( $\theta = 0$ ) has a response maxima at the center of the rectangle,  $(x, y) = (0, 0)$ , on a frequency which is specific to the width of the rectangle, the fundamental frequency [6], as illustrated in Figure 1 for a rectangle of width  $w_1 = 1$  and length  $w_2 = \infty$  (maxima at  $f = 0.5$ ). The harmonics of the fundamental frequency are also present, but the response for the harmonics can be eliminated with a proper selection of the parameter  $\gamma$ . In Figure 1, it can be seen that the effect of the first harmonic vanishes for  $\gamma \approx 0.58$ . The normaliza-

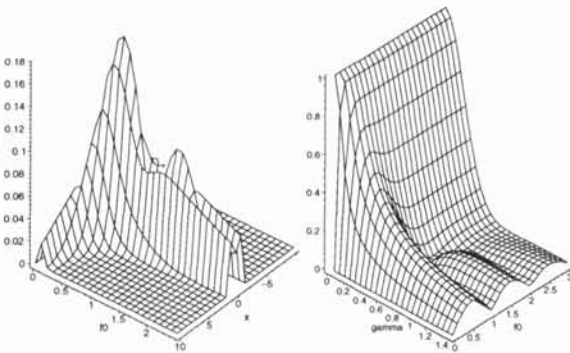


Figure 1: Normalized response for rectangle ( $w_1 = 1, w_2 = \infty$ ).

tion factor  $\eta$  controls the effective width of the modulating Gaussian perpendicular to the wave, orthogonal direction to the  $\gamma$ . In Figure 2, the response for the rectangle ( $w_1 = w_2 = 1$ ) starts to decrease rapidly for values  $\eta > 0.2$ , which is evident since the filter envelope

spreads over a significantly larger area than it is sufficient for the rectangle along that direction. Finally,

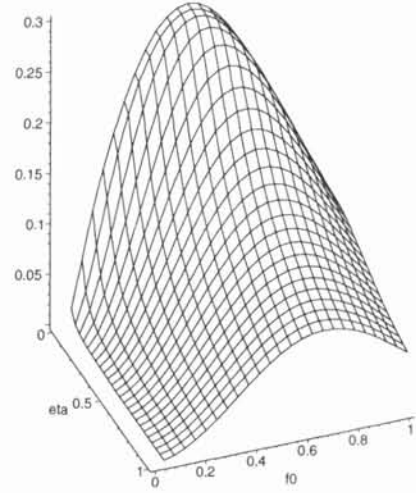


Figure 2: Normalized response for rectangle ( $w_1 = w_2 = 1$ ).

the effect of the orientation  $\theta$  is demonstrated in Figure 3 for a rectangle of width  $w_1 = 1$  and infinite length  $w_2 = \infty$ . Clearly, as the Gabor filter tuned on the correct frequency is rotated away from the direction of the feature ( $w_1$ ) the response gradually decreases. All

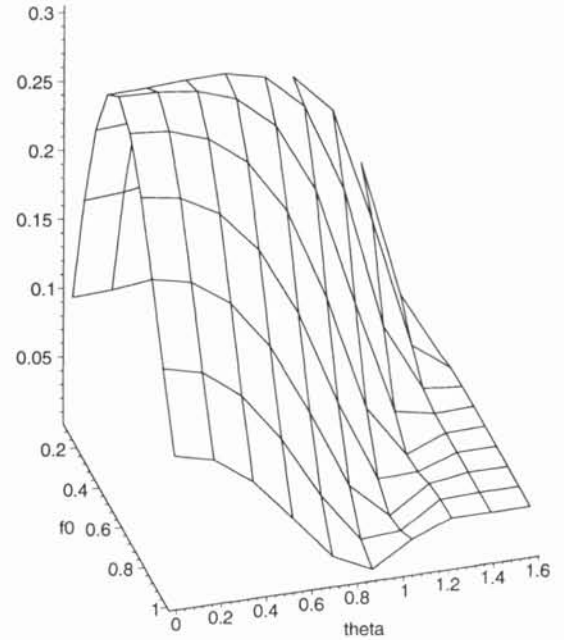


Figure 3: Normalized response for rectangle ( $w_1 = 1, w_2 = \infty$ ).

examples shown in Figures 1, 2, and 3 express smooth behavior of the response as function of the filter parameters.

Based on the shown results and studies on shiftability [12], it seems that smooth behavior is guaranteed for Gabor filters in terms of spatial location and filter parameters. In practice, applications utilizing the Gabor filter should not violate the restrictions (5), (6), and (7), otherwise the results of the analysis in the continuous domain do not apply. The analysis of the response for a rectangle function indicates that smooth

behavior can be achieved for individual filters in terms of the filtering parameters. Next, experiments are presented to demonstrate that even for a suboptimal values of parameters, accurate and reliable results can be achieved.

### 3 Experiments

The global Gabor features were calculated for base images in Figure 4 to generate a histogram of lines in different orientations [8, 9]. A set of electrical symbols were used as base images and their randomly rotated variants were used in the classification. The classification was carried out by measuring a rotation invariant Euclidean distance [9] to all base classes and assigning the class with the smallest distance. All images in ran-



Figure 4: Electrical symbols.

dom rotations were perfectly matched with the filtering parameters  $\gamma = 1$ ,  $\eta = 1$ ,  $f = 0.056$  and the number of orientations of equally spaced filters  $N = 20$  (shown by dashed lines in the plots in Figure 5). To inspect the effect of the parameters, the classification experiment was repeated with varying the parameters  $\gamma$ ,  $\eta$ ,  $f$ , and  $N$ .

The selected frequency  $f$  is specific for each class of features, e.g., the fundamental frequencies for the object size inspection and high frequencies for the edge detection. The matching accuracy is illustrated in Figure 5(a) as a function of the frequency  $f$ . In this experiment, the matching accuracy was optimal on a frequency corresponding to line width of the symbols. However, the matching accuracy remained almost the same around the optimal frequency  $f \approx 0.056$ , and gradually decreased when the frequency was selected farther away from 0.056 as can be seen in Figure 5(a). On frequencies significantly different than 0.056, the feature does not clearly represent the line information. There is a certain number of orientations which are needed for successful recognition and above that more orientations do not provide additional information. Figure 5(b) shows that after 16 orientations, the recognition can be performed perfectly.

$\gamma$  and  $\eta$  were used to control the effective spatial inspection area of the feature, the envelope of the Gaussian. Normalization constants should be selected to provide a sufficiently large area where frequencies can be inspected as the uncertainty theorem states. For example,  $\gamma = \sqrt{2}$  provides an effective spatial area, the standard deviation of the Gaussian envelope, of exactly one wavelength  $1/f$  of the selected frequency  $f$ . Again, the selection of the normalization constants was not a critical consideration as demonstrated in Figures 5(c)-(d) but a suboptimal selection is sufficient when the constraints (5) and (6) are not violated.

### 4 Conclusions

In this study, the robustness of the Gabor features was studied in terms of the Gabor filtering parameters. First, the Gabor filter response was examined as a function of the filter parameters for a rectangle function representing a non-periodic feature. The results indicated that the filter response is insensitive to small variations of the parameters. The conducted experiment on electric symbols demonstrated the analytical results in practice. In addition, restrictions for bandwidth parameters were proposed for a proper Gabor filter construction in the discrete domain.

The Gabor filters can be selected to have an overlap along spatial dimensions in the input space to provide a smooth transition between the filter responses and this study implies that a smooth behavior can also be achieved for the response of a single filter.

It seems that the Gabor filters can be reliably used in low-level feature extraction in image processing, and thus, the upper layer image analysis and applications can be reliably implemented upon the Gabor features. In future work, the shiftability properties of Gabor filters should be examined in detail.

### Acknowledgements

The authors would like to thank ECSE (East Finland Graduate School in Computer Science and Engineering) for financial support.

### References

- [1] Alan Conrad Bovik, Marianna Clark, and Wilson S. Geisler. Multichannel texture analysis using localized spatial filters. *IEEE Transactions on Pattern Analysis and Machine Intelligence*, 12(1):55–73, January 1990.
- [2] Joachim Buhmann, Martin Lades, and Christoph von der Malsburg. Size and distortion invariant object recognition by hierarchical graph matching. In *IJCNN International Joint Conference on Neural Networks*, volume 2, pages 300–311, 1990.
- [3] Jian Chen, Yoshinobu Sato, and Shinichi Tamura. Orientation space filtering for multiple orientation line segmentation. *IEEE Transactions on Pattern Analysis and Machine Intelligence*, 22(5):417–429, May 2000.
- [4] Y. Hamamoto, S. Uchimura, K. Masamizu, and S. Tomita. Recognition of handprinted chinese characters using Gabor features. In *Third International Conference on Document Analysis and Recognition*, volume 2, pages 819–823, 1995.

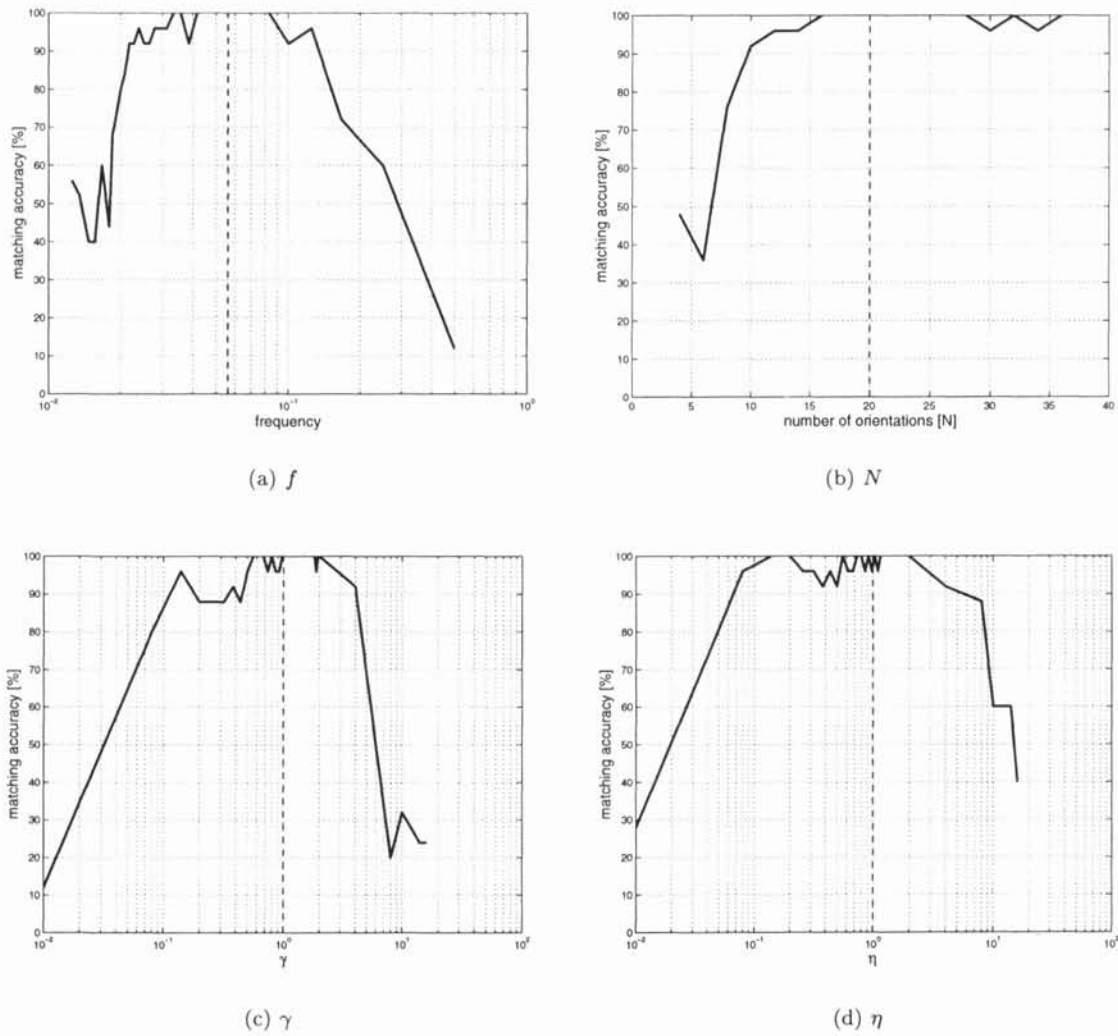


Figure 5: The dependence of matching accuracy on selection of parameter values.

- [5] Anil K. Jain and F. Farrokhnia. Unsupervised texture segmentation using Gabor filters. *Pattern Recognition*, 24(12):1167–1186, 1991.
- [6] J.-K. Kamarainen, V. Kyrki, and H. Kälviäinen. Fundamental frequency Gabor filters for object recognition. In *16th International Conference on Pattern Recognition ICPR2002*, volume 1, pages 628–631, Quebec, Canada, 2002.
- [7] J.-K. Kamarainen, V. Kyrki, and H. Kälviäinen. Noise tolerant object recognition using Gabor filtering. In *Proceedings of DSP2002 14th International Conference on Digital Signal Processing*, pages 1349–1352, Santorini, Greece, 2002.
- [8] V. Kyrki, J.-K. Kamarainen, and H. Kälviäinen. Content-based image matching using Gabor filtering. In *ACIVS'2001 3rd International Conference on Advanced Concepts for Intelligent Vision Systems Theory and Applications*, pages 45–49, Baden-Baden, Germany, July 2001.
- [9] V. Kyrki, J.-K. Kamarainen, and H. Kälviäinen. Invariant shape recognition using global Gabor features. In *12th Scandinavian Conference on Image Analysis*, pages 671–678, Bergen, Norway, June 2001.
- [10] Jouko Lampinen and Seppo Smolander. Self-organizing feature extraction in recognition of wood surface defects and color images. *International Journal of Pattern Recognition and Artificial Intelligence*, 10(2):97–113, 1996.
- [11] R. Mehrotra, K.R. Namuduri, and N. Ranganathan. Gabor filter-based edge detection. *Pattern Recognition*, 25(12):1479–1494, 1992.
- [12] Eero P. Simoncelli, William T. Freeman, Edward H. Adelson, and David J. Heeger. Shiftable multi-scale transforms. *IEEE Transactions on Information Theory*, 38(2):587–607, March 1992.